A computational hyperspectral structured light sheet microscope

Sébastien Crombez, Pierre Leclerc, Cédric Ray, Nicolas Ducros

A computational hyperspectral structured light sheet microscope

S Crombez[1,2], P Leclerc[1,2], C Ray[2], N Ducros[1],

[1] *Univ. Lyon, INSA-Lyon, UCB Lyon 1, UJM-Saint Etienne, CREATIS CNRS UMR 5220, Inserm U1206, F-69621, LYON, France*

[2] *Univ. Lyon, Université Claude Bernard Lyon 1, CNRS, Institut Lumière Matière, F-69622, Villeurbanne, France*

nicolas.ducros@creatis.insa-lyon.fr

Abstract:
We describe here a hyperspectral light sheet microscope that is based on beam shaping and image reconstruction. Our approach has no moving parts and can be easily combined with a standard microscope.

1. Introduction

As in *Jahr et al.* [1], we consider the acquisition of a four-dimensional (4D) hypercube $\Omega = (x, y, z, \lambda)$, where (x, y, z) is the voxel position, and λ is the wavelength. A single plane illumination microscope (SPIM) images the volume $f(x, y, z)$ by acquiring 2D optical sections (x, y) sequentially at multiples $z \in \{z_\ell\}_{1 \leq \ell \leq L}$. Let $f^\ell(x, y, \lambda)$ denote the optical section at z_ℓ.

2. Proposed methodology

2.1. 1D modulation

In standard SPIM, the illumination sheet p is designed to be uniform in the 2D plane (x, y). Here, we propose to modulate the illumination along the x-axis and use a cylinder lens to focus the light on the slit of a spectrometer, which is oriented along the y-axis. Measurements are repeated for a set of modulation patterns $\{p_k\}_{1 \leq k \leq K}$, which leads to the set of measurements $\{m_k^\ell(y, \lambda)\}_{1 \leq k \leq K}$ that can be modelled as $m_k^\ell(y, \lambda) = \int f^\ell(x, y, \lambda) p_k(x) \mathrm{d}x$. Each of the L optical sections are acquired independently by traversing the sample. In a discrete setting, we denote $\mathbf{m}_\lambda^y \in \mathbb{R}^{N_k}$ as the measurements obtained for all of the modulation patterns at a given λ and vertical position y, where N_k is the number of modulation patterns. The discrete forward model leads to $\mathbf{m}_\lambda^y = \mathbf{P}\mathbf{f}_\lambda^y$, $\forall(\lambda, y)$ where $\mathbf{P} \in \mathbb{R}^{N_k \times N_x}$ is the modulation matrix, and $\mathbf{f}_\lambda^y \in \mathbb{R}^{N_x}$ is the optical profile at vertical position y and wavelength λ. Note that the number of pixels along the (compressed) x-axis is denoted by N_x. When $N_k = N_x$, and assuming that $\mathbf{P}$ is an orthogonal matrix (e.g., Hadamard, Fourier, wavelets patterns), the optical profile can be reconstructed by $\mathbf{f}_\lambda^y = \mathbf{P}^\top \mathbf{m}_\lambda^y$, $\forall(\lambda, y)$. As the experimental patterns differ from the theoretical ones, we reconstruct the hypercube using the Tikhonov regularized least square solution

$$\hat{\mathbf{f}}_\lambda = (\mathbf{A}^\top \mathbf{A} + \alpha \mathbf{I})^{-1} \mathbf{A}^\top \mathbf{m}_\lambda \tag{1}$$

where $\mathbf{A}$ contains the experimental patterns.

2.2. Experimental set-up

Our optical system is shown in Fig. 1. It is fed by two continuous wave lasers that illuminate a digital micro-mirror device (DMD) that can shape the beam by reflecting only some part of it. The modulated beam is fed to a modified OpenSPIM (Pitrone *et al.* [2])) set-up to generate the structured light sheet that illuminates the sample with a given modulation pattern. The light emitted by the sample can be sent to two detection arms. A standard arm provides classical SPIM imaging, while the hyperspectral arm focuses the light on the slit of the spectrometer, to perform hyperspectral SPIM.

3. Results

To assess our set-up for the unmixing of two fluorophores, we measured a hydra sample labelled with two fluorophores (Superfloder GFP for the skin, DsRed2 for the inner tissues), as shown in Fig. 2a. We measured the same slice of the hydra tail (see Fig. 2b) using both arms. In Fig. 2d, we superimpose the reconstruction that corresponds

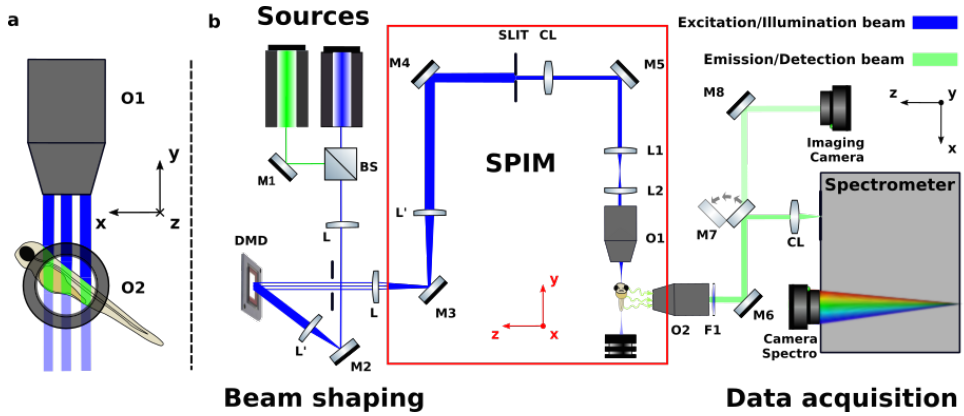

Fig. 1. (a) Schematic of the structured light sheet illumination. (b) Scheme of the computational hyperspectral SPIM demonstrator (chSPIM) with a control arm that allows classical SPIM imaging.

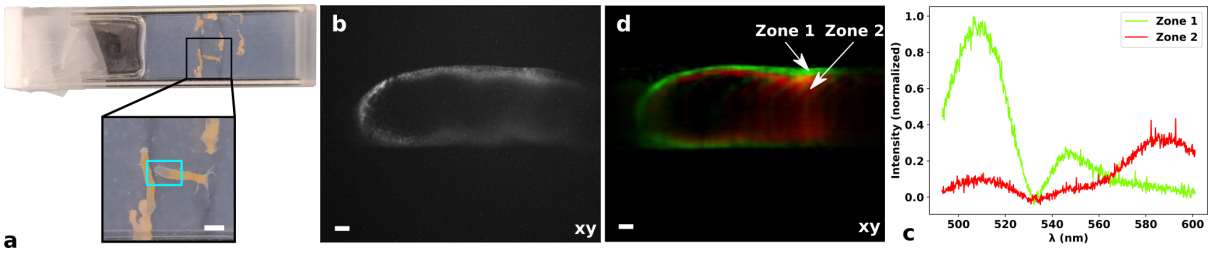

Fig. 2. Comparison of conventional and hyperspectral imaging of a two-colour specimen of a hydra, using Superfolder GFP ($\lambda^{\text{em}} = 510$ nm) and DsRed2 ($\lambda^{\text{em}} = 587$ nm). (a) Picture of the sample. The cyan box indicate the SPIM field of view. Scale bar, 1 mm. (b) SPIM acquisition. Scale bar, 100 μm. (c) Spectrum of zones 1 and 2. (d) chSPIM acquisition; green: reconstruction for $\lambda \in$ [493 - 527] nm; red: reconstruction for $\lambda \in$ [576-601] nm. Scale bar, 100 μm.

to the emission of the GFP (green channel) and that corresponds to the DsRed (red channel). Fig. 2c shows the plot of the emission spectrum of a pixel taken in the skin area, and another in the inner tissue.

The reconstruction of the compressed dimension (i.e., x-axis) remains the main challenge, as can be seen by comparing the SPIM-arm and the chSPIM-arm images. Here, we only consider 64 modulation patterns to encode the x-axis spatial dimension, while the SPIM arm has 2560 pixels along this dimension. Other limiting factors include beam shaping while maintaining high spatial frequency and increasing the imaging rate.

4. Conclusion

We propose a computational hyperspectral SPIM set-up based on a DMD that generates a structured light sheet. We demonstrate the acquisition of a full hypercube of a two-colour sample with high spectral resolution. In future studies, we will work on improving the spatial resolution while maintaining the spectral resolution.

References

1. W. Jahr, B. Schmid, C. Schmied, F. Fahrbach, and J. Huisken, "Hyperspectral light sheet microscopy," Nat. Communications **6**, 7990 (2015)
2. Pitrone P. G., Schindelin J., Stuyvenberg L., Preibisch S., Weber M.; Eliceiri K. W., Huisken J., Tomancak P. "OpenSPIM: an open access light sheet microscopy platform", Nat. Methods **10**, 598 599 (2013).